AGU PUBLICATIONS

Radio Science

RESEARCH ARTICLE
10.1002/2017RS006507

Special Section:
URSI General Assembly and Scientific Symposium (2017)

Wireless Sensor Network for Radiometric Detection and Assessment of Partial Discharge in High-Voltage Equipment

D. W. Upton[1], B. I. Saeed[1], P. J. Mather[1], P. I. Lazaridis[1], M. F. Q. Vieira[2], R. C. Atkinson[3], C. Tachtatzis[3], M. S. Garcia[3], M. D. Judd[4], and I. A. Glover[1]

[1]Department of Engineering and Technology, University of Huddersfield, Huddersfield, UK, [2]Departamento de Engenharia Eletrica, Universidade Federal de Campina Grande, Campina Grande, Brazil, [3]Department of Electronic and Electrical Engineering, University of Strathclyde, Glasgow, UK, [4]High Frequency Diagnostics and Engineering Ltd., Glasgow, UK

Key Points:
- A low-power wireless sensor network for noninvasive high-voltage plant condition monitoring
- The network utilizes radiometric UHF partial discharge for detection and measurement, requiring no physical connection to HV plant
- A fully scalable early warning system for locating high-voltage insulation faults over a large monitoring area

Correspondence to:
D. W. Upton,
d.w.upton@hud.ac.uk

Citation:
Upton, D. W., Saeed, B. I., Mather, P. J., Lazaridis, P. I., Vieira, M. F. Q., Atkinson, R. C., et al. (2018). Wireless sensor network for radiometric detection and assessment of partial discharge in high-voltage equipment. *Radio Science*, *53*. https://doi.org/10.1002/2017RS006507

Received 23 NOV 2017
Accepted 6 MAR 2018
Accepted article online 10 MAR 2018

©2018. The Authors.
This is an open access article under the terms of the Creative Commons Attribution-NonCommercial-NoDerivs License, which permits use and distribution in any medium, provided the original work is properly cited, the use is non-commercial and no modifications or adaptations are made.

Abstract Monitoring of partial discharge (PD) activity within high-voltage electrical environments is increasingly used for the assessment of insulation condition. Traditional measurement techniques employ technologies that either require off-line installation or have high power consumption and are hence costly. A wireless sensor network is proposed that utilizes only received signal strength to locate areas of PD activity within a high-voltage electricity substation. The network comprises low-power and low-cost radiometric sensor nodes which receive the radiation propagated from a source of PD. Results are reported from several empirical tests performed within a large indoor environment and a substation environment using a network of nine sensor nodes. A portable PD source emulator was placed at multiple locations within the network. Signal strength measured by the nodes is reported via WirelessHART to a data collection hub where it is processed using a location algorithm. The results obtained place the measured location within 2 m of the actual source location.

1. Introduction

Partial discharge (PD) is a fault that occurs within the insulation of high-voltage (HV) plant such as cables, switchgear and transformers. PD is defined by the International Electrotechnical Commission (IEC) standard as "localized electrical discharge that only partially bridges the insulation between conductors and which can or cannot occur adjacent to a conductor. Partial discharges are in general a consequence of local electrical stress concentrations in the insulation or on the surface of the insulation. Generally, such discharges appear as pulses having a duration of much less than 1 microsecond" (IEC International Standard 60270, 2000). The detection of PD activity permits the condition of HV plant to be assessed and enables insulation defects to be detected and located, and corrective action to be taken, before catastrophic failure (flashover) occurs (de Souza Neto et al., 2013). The detection and measurement of PD is a widely used technique for the assessment of HV plant (Reid et al., 2011) and many techniques have been developed utilizing both contact and wireless technologies.

This paper presents the progress made toward implementing a versatile, fully-scalable, wireless sensor network (WSN) intended to monitor HV plant within an electricity substation, previous developments to the project have been reported in Zhang, Neto, et al. (2015), Zhang, Upton, et al. (2015), Upton et al. (2017), and Jaber et al. (2017). The WSN utilizes received signal strength (RSS) of the electromagnetic wave radiated by a source of PD. A WSN provides benefits over traditional wired PD detection techniques such as installation without taking plant off-line, ease of reconfiguration, and graceful system degradation in the event of node failure. For the WSN to be a practical, fully scalable solution to PD monitoring, the sensor nodes must be low cost, low power, and able to detect PD radiation with intensity of engineering interest at a range of at least 10 m.

Traditional radiometric techniques for the detection and location of PD sources, such as time of arrival and time difference of arrival (Judd, 2008; Li et al., 2017; Moore et al., 2003; Portugues et al., 2009; Robles et al., 2016; Zhu et al., 2016, 2017), employ technologies that require high-speed data acquisition and relatively large amounts of data processing, as well as synchronization between nodes, making the design of the sensor nodes complex and costly. An RSS-only monitoring and location technology provides a simpler and cheaper approach, which can be fully scalable and requires no synchronization between nodes (de Souza

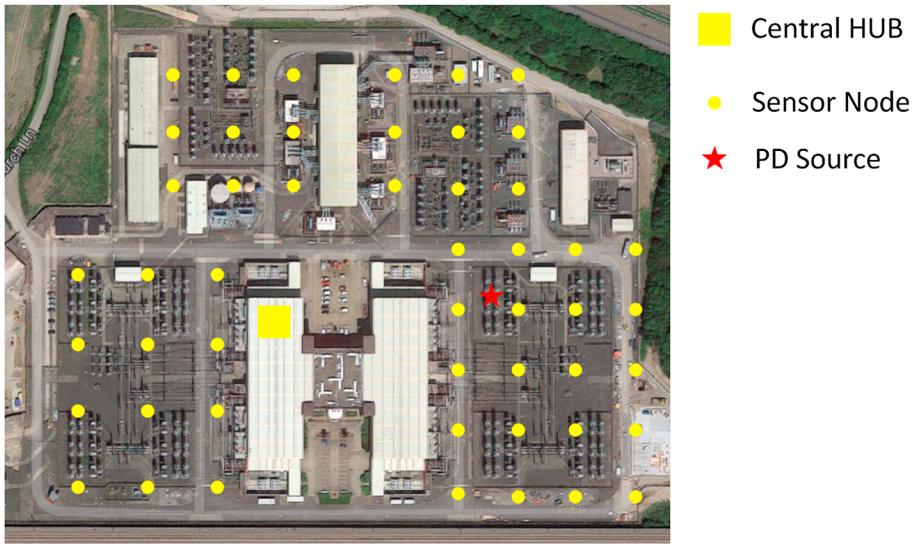

Figure 1. Conceptual partial discharge (PD) wireless sensor network (photo copyright Google™).

Neto et al., 2012). Previous RSS PD measurement systems have been developed (Baker et al., 2009, 2010; Huang et al., 2017) that utilize radio-frequency (RF) envelope-tracking power detectors to reduce the required sampling rate; however, data acquisition in excess of 10 MSa/s is still required to process radiometric PD signals.

2. Partial Discharge Wireless Sensor Network

The PD WSN is composed of an array of radiometric sensor nodes which all communicate to a central data collection hub. A conceptual layout of the proposed PD WSN, superimposed over an overhead photograph of a typical medium voltage substation in the UK, is shown in Figure 1.

To avoid the measurements of PD intensity being inflated by communication signals, the measurement is limited to frequencies below 320 MHz, where the majority of PD activity occurs. Notch filters are also incorporated to remove narrowband interference (in particular broadcast signals) below this frequency.

Data are transmitted from sensor nodes to the data collection hub in the 2.4 GHz industrial, scientific and medical (ISM) band to avoid interfering with the measurement of PD activity. The WirelessHART transmission protocol used is resilient to the harsh electromagnetic environment. It supports a mesh topology and features self-configuring, self-healing functions.

2.1. Sensor Nodes

The sensor node, shown in Figure 2, consists of four subsystems: an RF front end, a signal conditioning unit, a microcontroller, and a WirelessHART unit. A dipole antenna is used as the receiving radiometer antenna, because an omnidirectional radiation pattern is desirable, coupled through a 4:1 balun to increase the bandwidth. Experimental data suggest that the typical spectra for various radiometric PD types is between 50 and

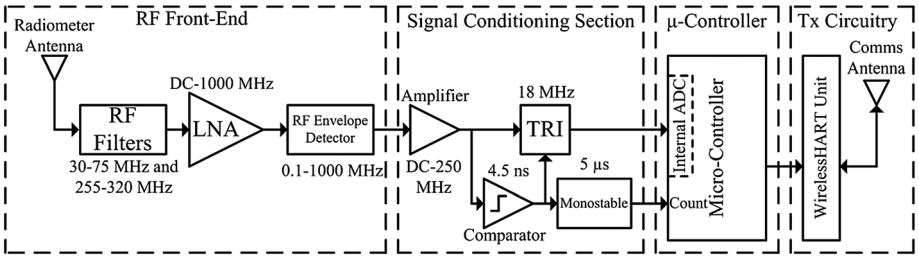

Figure 2. Wireless sensor node block diagram. LNA = low-noise amplifier; TRI = transistor-reset integrator; ADC = analog-to-digital converter.

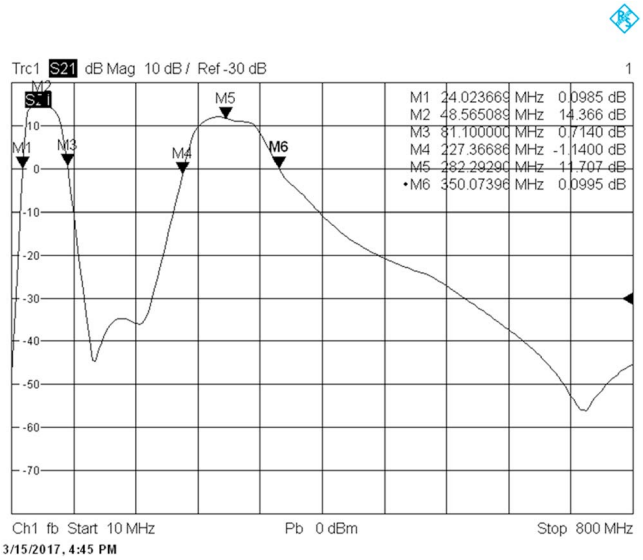

Figure 3. RF front end frequency response.

800 MHz, with the majority below 300 MHz (Albarracín et al., 2016; Hoshino et al., 2001; Jaber et al., 2017; Robles et al., 2012, 2013; Tenbohlen et al., 2008; Xiao et al., 2009); therefore, a sensor bandwidth in this region was selected. The receiving antenna is connected to the RF front end, which contains a band-pass filter for the 30–320 MHz band, a band-stop filter for the 75–255 MHz band, an ADL5530 low-noise amplifier, and an LTC5507 RF envelope detector. The filters remove interference, such as FM, private mobile radio, digital radio, and TV, that may be present in the monitored band. There are two resulting pass-bands from 30 to 75 MHz and from 255 to 320 MHz, with a midband gain between 11.7 and 14.4 dB and a measured noise figure of 5–7 dB. Figure 3 shows the frequency response of the RF front end.

The envelope detector reduces the signal bandwidth by removing the RF component of the PD signal, leaving only the envelope. The envelope detected signal is applied to the signal conditioning circuit, Figure 4, which provides further amplification, along with a count for each received PD event, before integrating the envelope detected pulse.

The envelope-detected signal is AC coupled through filter C_1 and R_1 and then amplified by the noninverting amplifier U_1 set to a gain of three. The amplified signal is then applied to a high-speed comparator, set to a 4 mV threshold voltage, and a transistor-reset integrator (TRI). The TRI is switched between two modes, integration and hold, via switches S_1 and S_2. When the received PD event is approximately above 1.3 mV, comparator U_3 outputs a logic high signal, actuating S_1 and activating the integration mode. S_2 is actuated at the same time in order to compensate for the charge injection of S_1. Signals below the comparator threshold, such as envelope-detected noise, are prevented from creating a constant rise in integrator output voltage. The comparator also counts the number of received (individual) PD events by activating the monostable circuit, feeding a logic high level to the microcontroller. The monostable is set for a 5 μs duration, ensuring that the microcontroller has enough time to acknowledge the signal. Once the signal voltage drops below the threshold, integration is stopped and the output of the TRI is thus held at a constant level. The integrator reset function is achieved through comparator U_4 and transistors Q_1 and Q_2. When the precision integrator output voltage exceeds the −1.5 V threshold level of U_2 the output drives high, activating Q_1 and Q_2. Q_1 discharges

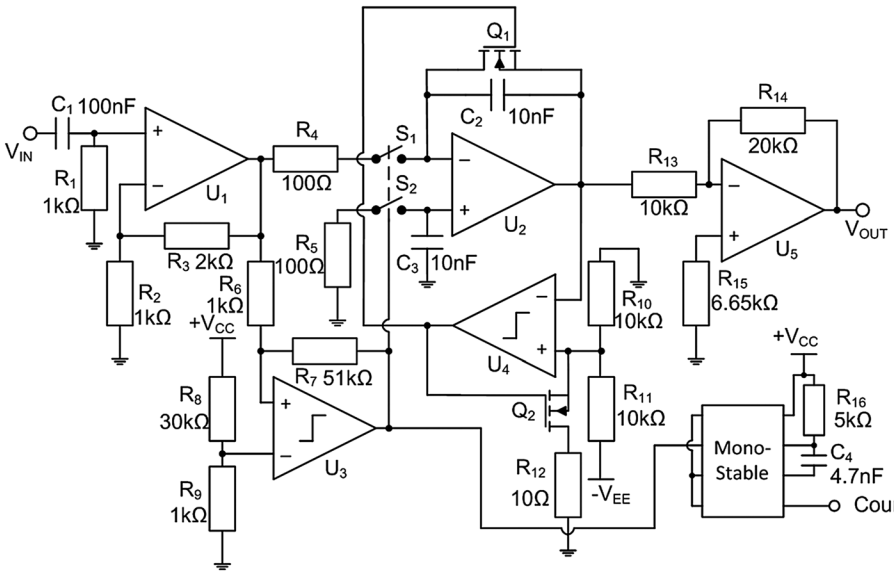

Figure 4. Signal conditioning circuit diagram.

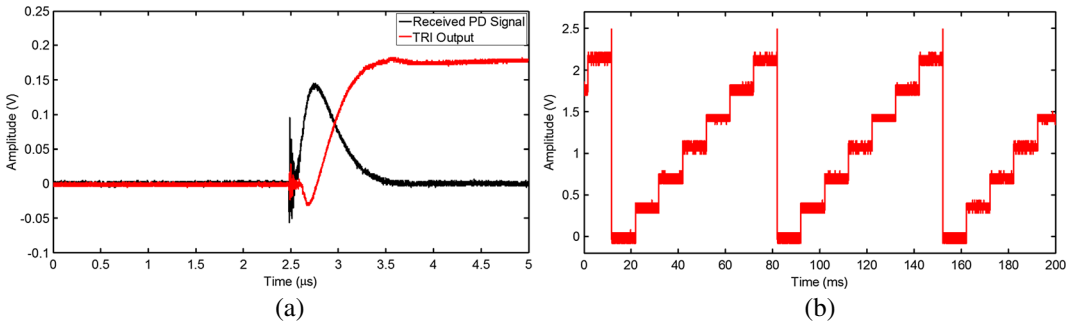

Figure 5. (a) RF envelope detector and transistor-reset integrator (TRI) output for a single partial discharge (PD) event and (b) TRI output for multiple events.

the feedback capacitor C_1, effectively resetting the integrator, while Q_2 adjusts the threshold of comparator U_4 to near 0 V, ensuring that the integrator is fully reset. The inverting (2 times) amplifier U_5 inverts the output of the integrator to a positive-going voltage and scales it to the 3 V power supply range to ensure that the maximum analog-to-digital converter dynamic range is utilized.

The TRI reduces the bandwidth of a single envelope-detected signal to a DC voltage level, resulting in a staircase signal at the output of the TRI for multiple received PD events. It provides an output which is a metric of accumulated PD activity. Figure 5a shows the outputs on an expanded timescale of the RF envelope detector and the TRI after a single emulated PD event, and Figure 5b shows the output of the TRI for multiple events from a PD calibration source with a 10 ms repetition rate.

The signal held at the output of the TRI is sampled once by the internal analog-to-digital converter of a microcontroller when the signal from comparator U_3 is applied to a digital "count" input. The strength (i.e., integral) of each detected PD pulse is determined by taking the difference between the current and previous samples. The samples are then acquired and averaged by the microcontroller over a 1 s period. The average integrated signal and the count value are transmitted to the data collection hub via the WirelessHART transceiver. The signals are then processed to locate the source of PD. The integrator output step size is a measure of the received PD signal power at the terminals of the receiving antenna. A small number of pulses per reset period indicate a strong received signal, while a large number of pulses per reset period indicate a weak received signal.

2.2. Sensor Node Calibration

A commercial HVPD pC (picocoulomb) charge injection pulse generator was used to calibrate the sensor nodes. The device provides pulses from 1 pC to 100 nC (100,000 pC) with selectable pulse repetition rate (100, 120, and 400 Hz). Figure 6 shows a 1 nC pulse generated by the calibrator into a 50 Ω load.

The calibrator was set to generate a 1 nC pulse with a repetition rate of 100 Hz and connected via an attenuator to the front end of the sensor node. To present different power levels at the front end, the attenuator value was changed in discrete steps of 3 dB or 4 dB. With each attenuator setting the signal peak power was measured at the front end and the output of the TRI was sampled and transferred to a PC to calculate the average step size. The relationship between signal peak power and TRI step size, shown in Figure 7, is used to calculate the received peak power using linear interpolation. The dual slope is due to gain compression within the LTC5507 detector to increase dynamic range at higher input powers.

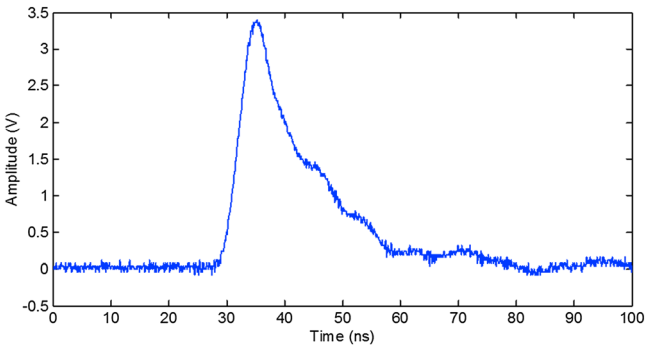

Figure 6. Output voltage pulse of the HVPD calibrator set to 1 nC.

2.3. Location Algorithm

The source localization is based on a location algorithm that relies on RSS (Xu et al., 2014). The algorithm uses the simple propagation model

$$P_R = P_0 - 10n \log_{10} d_i \quad (1)$$

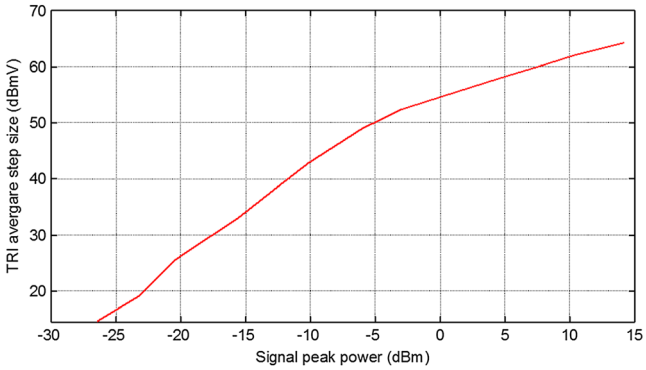

Figure 7. Transistor-reset integrator average step size versus signal peak power.

where P_R, P_0, d_i, and n are the received power, transmitted power, distance from the source, and path loss index, respectively. The location algorithm is executed as follows:

1. Initial estimation is done assuming a global path loss index, n, for all sensor nodes.
2. The ratios of power received is calculated for sensor node pairs to generate a loci of source location.
3. Estimated source locations are generated at each intersecting loci.
4. The mean spatial location is calculated from all estimated locations for a single value of n.
5. The calculation is then repeated for all plausible values of n (1–7).
6. The final mean location estimate is then selected based on the least mean squares value.

Although the location algorithm is based on the simple propagation model described, it has been found to perform to an acceptable accuracy for radiometric PD (within 2 m) for the majority of experimental work performed thus far. However, for WSN operation within harsher electromagnetic environments, a high-performance location algorithm would be utilized (Fresno et al., 2017; Iorkyase et al., 2017).

3. Results

Two tests were performed, one in an indoor sports hall and one in a more realistic environment at the Power Networks Demonstration Centre (PNDC) near Glasgow, Scotland. Possible electromagnetic interference within the sensor measurement bandwidth ranges from FM radio, digital audio broadcasting (DAB), corona discharges, and fluorescent lamp ignition (Albarracín et al., 2015). Since FM and DAB are removed via the front end RF filtering these sources were not an issue in either test. No equipment emitting corona discharge was present during the sports hall test, and the plant equipment at the PNDC was not energized during the test. Finally, although fluorescent lights were present in the sports hall, the distance between the sensor nodes and the ceiling mounted lights was far enough to ensure no interference was received, and no fluorescent lights were present during the PNDC test. Interference in the UHF band, such as DVB-T and LTE/GSM, was outside of the measurement band of the sensors.

3.1. Indoor Test

A nine-node sensor network was used for the indoor test. The sensors were placed in a square grid with 9 m spacing, as shown in Figure 8. The HVPD pC calibrator connected to Aaronia BicoLOG 20100E biconical

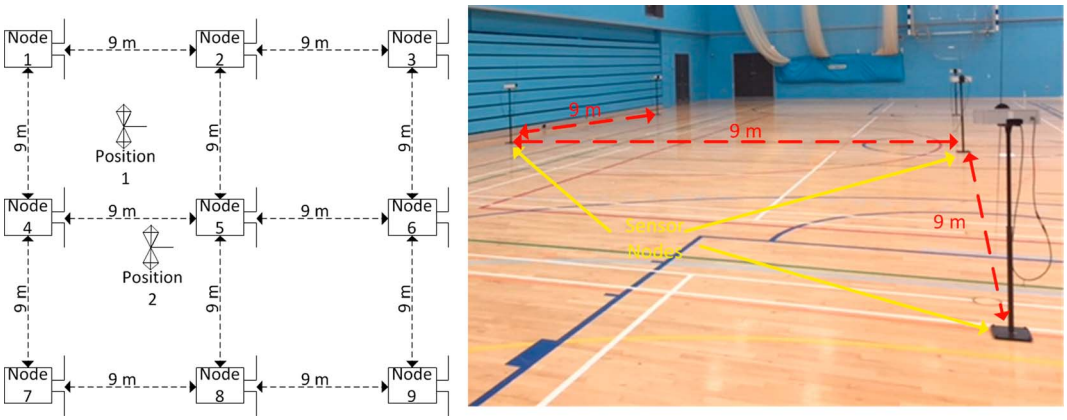

(a) (b)

Figure 8. (a) Partial discharge wireless sensor network layout and (b) photograph of the test space.

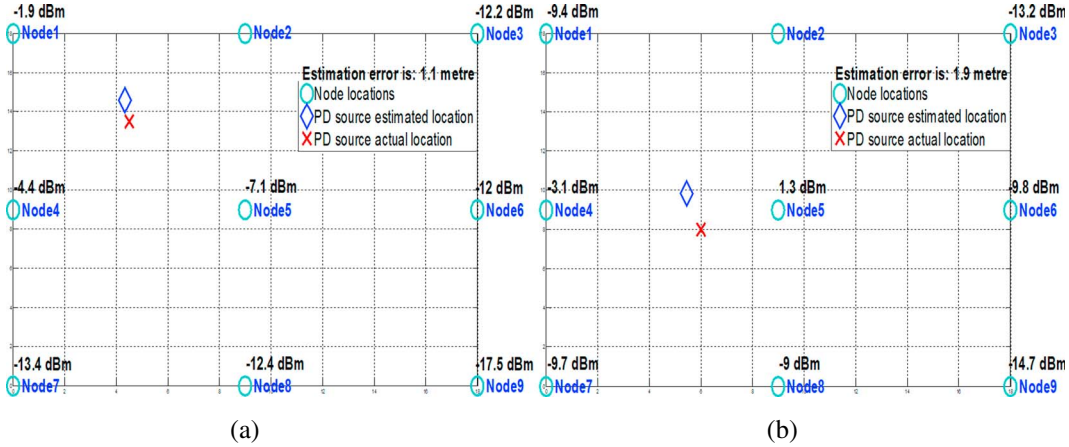

Figure 9. Estimated location of the partial discharge (PD) source (a) Position 1 and (b) Position 2.

antenna was used as a PD emulator to generate the signal to be located. The PD emulator was set to generate 10 nC pulses at a repetition rate of 100 Hz.

The PD source was placed in two different locations, labeled as Position 1 and Position 2 in Figure 8a. The sensors were programmed to collect data for a duration of 1 s. For each location the test was repeated five times. No data are presented for node 2 because it malfunctioned during the test. As can be seen in Figure 9, the PD source locations were estimated approximately with an error of 1.1 and 1.9 m for Positions 1 and 2, respectively.

3.2. PNDC Substation Test

The second test was conducted using the same nine-node network at the PNDC. The PNDC provided an environment equivalent to a substation, with switchgear, transformers, and earthed metal shielding; however, the PNDC HV network was not energized during the test. Sensors were spaced at intervals of 8 m, as shown in Figure 10, due to space constrictions within the PNDC.

As with the indoor test, the HVPD pC calibrator was used to generate a 10 nC emulated source of PD at a repetition rate of 100 Hz. The PD calibrator was placed in two locations (PD Source 1 and PD Source 2) , and the resulting received powers for each node were transmitted to the central hub, where the location algorithm was then applied. The results in Figure 11 show an error of 1.2 and 1.0 m for Sources 1 and 2, respectively.

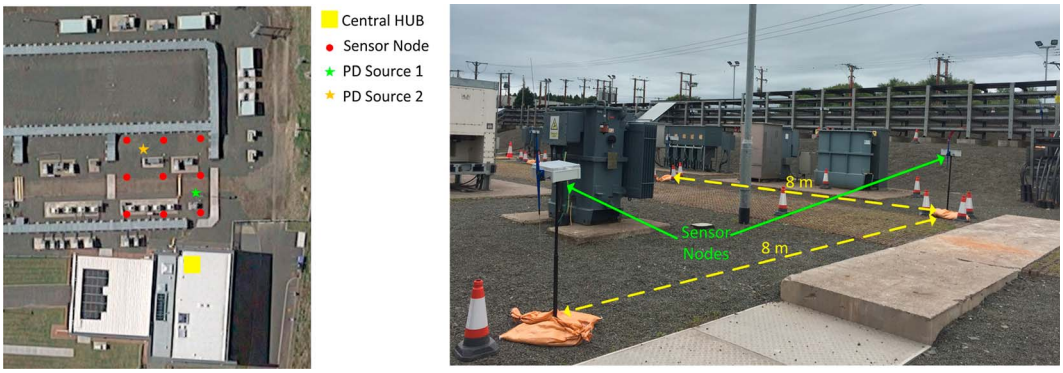

Figure 10. (a) Overhead view of the Power Networks Demonstration Centre WSN layout. (b) Sensors in the Power Networks Demonstration Centre test space. PD = partial discharge.

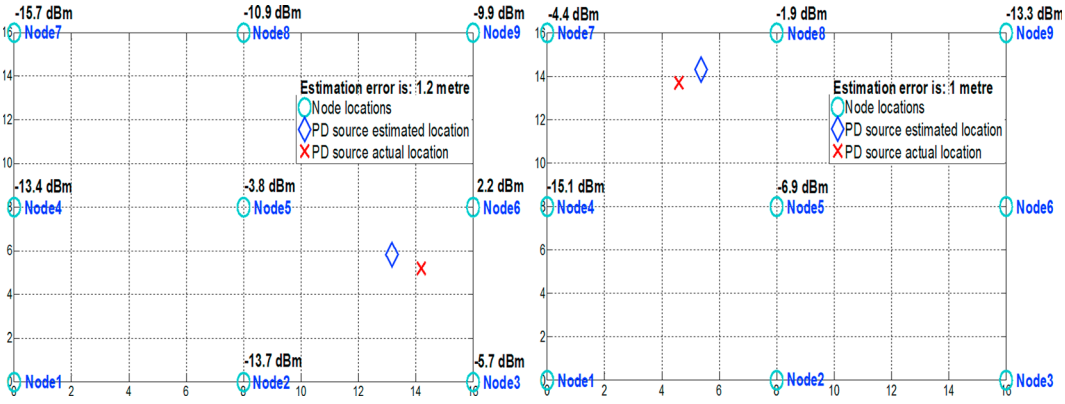

(a) (b)

Figure 11. Estimated location of the partial discharge (PD) source for (a) PD Source 1 and (b) PD Source 2.

4. Conclusion

A real-time radiometric WSN system for monitoring and locating PD sources has been designed, implemented, and tested within an indoor and substation environment, and an RSS-based location algorithm has been demonstrated to successfully locate an emulated source of PD. The results obtained from testing within the PNDC demonstrate that the WSN is capable of detecting and measuring PD activity within a substation environment with useful accuracy.

Acknowledgments
This work was supported by the U.K. Engineering & Physical Sciences Research Council under grant EP/J015873**.** The data required to reproduce the results included are available from the University of Huddersfield repository, located at http://eprints.hud.ac.uk/id/eprint/34351/.

References

Albarracín, R., Ardila-Rey, J. A., & Mas'ud, A. A. (2016). On the use of monopole antennas for determining the effect of enclosure of a power transformer tank in partial discharges electromagnetic propagation. *Sensors*, *16*(12), 1–18. https://doi.org/10.3390/s16020148

Albarracín, R., Robles, G., Martínez-Tarifa, J. M., & Ardila-Rey, J. (2015). Separation of sources in radiofrequency measurements of partial discharges using time-power ratio maps. *ISA Transactions*, *58*, 389–397. https://doi.org/10.1016/j.isatra.2015.04.006

Baker, P. C., Judd, M. D., & McArthur, S. D. J. (2010). A frequency-based RF partial discharge detector for low-power wireless sensing. *IEEE Transactions on Dielectrics and Electrical Insulation*, *17*(1), 133–140. https://doi.org/10.1109/TDEI.2010.5412011

Baker, P. C., Stephen, B., Judd, M. D., & McArthur, S. D. J. (2009). *Development of an integrated low-power RF partial discharge detector*. Paper presented at IEEE Electrical Insulation Conference, Montreal QC, Canada. https://doi.org/10.1109/EIC.2009.5166356

de Souza Neto, J. M. R., de Macedo, E. C. T., da Rocha Neto, J. S., Vieira, M. F., Glover, I. A., Judd, M. D., et al. (2013). *Plausability of incoherent detection for radiometric monitoring of insulation integrity in HV substations*. Paper presented at Loughborough Antennas and Propagation Conference (LAPC'13), Loughborough, UK. doi: 978–1–4799-0091-6

de Souza Neto, J. M. R., Macedo, E. C. T., da Rocha Neto, J. S., Da Costa, E. G., Bhatti, S. A., & Glover, I. A. (2012). Partial discharge location using unsynchronized radiometer network for condition monitoring in HV substations—A proposed approach. *Journal of Physics Conference Series*, *364*(1), 1–11. https://doi.org/10.1088/1742-6596/364/1/012053

Fresno, J. M., Robles, G., Martinez-Tarifa, J. M., & Stewart, B. G. (2017). Survey on the performance of source localization algorithms. *Sensors*, *17*(12), 1–25. https://doi.org/10.3390/s17112666

Hoshino, T., Kato, K., Hayakawa, N., & Okubo, H. (2001). A novel technique for detecting electromagnetic wave caused by partial discharge in GIS. *IEEE Transactions on Power Delivery*, *16*(4), 545–551. https://doi.org/10.1109/61.956735

Huang, W., Zhang, C., Dong, M., & Zhou, J. (2017). *Research on partial discharge monitoring system of switchgear based on wireless distributed TEV sensors*. Paper Presented at 1st International Conference on Electrical Materials and Power Equipment (ICEMPE). Xi'an, China. https://doi.org/10.1109/ICEMPE.2017.7982180

IEC International Standard 60270 (2000). *High voltage test techniques—Partial discharge measurements*. Geneva, Switzerland: International Electrotechnical Commission (IEC).

Iorkyase, E. T., Tachtatzis, C., Lazaridis, P., & Glover, I. A. (2017). Radio location of partial discharge sources: A support vector regression approach. *IET Science, measurement & Technology*, *12*(2), 230–236. https://doi.org/10.1049/iet-smt.2017.0175

Jaber, A. A., Lazaridis, P. I., Moradzadeh, M., Glover, I. A., Zaharias, Z. D., Vieira, M. F. Q., et al. (2017). Calibration of free-space radiometric partial discharge measurements. *IEEE Transactions on Dielectrics and Electrical Insulation*, *24*(5), 3004–3014. https://doi.org/10.1109/TDEI.2017.006730

Judd, M. D. (2008). *Radiometric partial discharge detection*. Paper presented at International Conference on Condition Monitoring and Diagnosis, Beijing, China. https://doi.org/10.1109/CMD.2008.4580457

Li, P., Zhou, W., Yang, S., Liu, Y., Tian, Y., & Wang, Y. (2017). Method for partial discharge localisation in air-insulated substations. *IET Science, Measurement & Technology*, *11*(3), 331–338. https://doi.org/10.1049/iet-smt.2016.0251

Moore, P. J., Portugues, I., & Glover, I. A. (2003). *A nonintrusive partial discharge measurement system based on RF technology*. Paper presented at IEEE Power Engineering Society General Meeting (IEEE Cat. No.03CH37491), Toronto ON, Canada. https://doi.org/10.1109/PES.2003.1270372

Portugues, I. E., Moore, P. J., Glover, I. A., Johnstone, C., McKosky, R. H., Goof, M. B., & van der Zel, L. (2009). RF-based partial discharge early warning system for air-insulated substations. *IEEE Transactions on Power Delivery*, *24*(1), 20–29. https://doi.org/10.1109/TPWRD.2008.2005464

Reid, A. J., Judd, M. D., Fouracre, R. A., Stewart, B. G., & Hepburn, D. M. (2011). Simultaneous measurement of partial discharges using IEC60270 and radio-frequency techniques. *IEEE Transactions on Dielectrics and Electrical Insulation*, *18*(2), 444–455. https://doi.org/10.1109/TDEI.2011.5739448

Robles, G., Fresno, J. M., Sánchez-Fernández, M., & Martínez-Tarifa, J. (2016). Antenna deployment for the localization of partial discharges in open-air substations. *Sensors*, *16*(12), 9882–9898. https://doi.org/10.3390/s16040541

Robles, G., Martínez-Tarifa, J. M., Rojas-Morena, M. V., Albarracín, R., & Ardila-Rey, J. (2012). *Antenna selection and frequency response study for UHF detection of partial discharges*. Paper Presented at IEEE International Instrumentation and Measurement Technology Conference (I2MTC), Graz, Austria. https://doi.org/10.1109/I2MTC.2012.6229440

Robles, G., Sánchez-Fernández, M., Albarracín, R., Rojas-Morena, M. V., Rajo-Iglesias, E., & Martínez-Tarifa, J. M. (2013). Antenna parametrization for the detection of partial discharges. *IEEE Transactions on Instrumentation and Measurement*, *62*(5), 932–941. https://doi.org/10.1109/TIM.2012.2223332

Tenbohlen, S., Denissov, D., Hoek, S. M., & Markalous, S. M. (2008). Partial discharge measurement in the ultra high frequency (UHF) range. *IEEE Transactions on Dielectrics and Electrical Insulation*, *15*(6), 1544–1552. https://doi.org/10.1109/TDEI.2008.4712656

Upton, D. W., Saeed, B. I., Khan, U., Jaber, A., Mohamed, H., Mistry, K., et al. (2017). *Wireless sensor network for radiometric detection and assessment of partial discharge in HV equipment*. Paper presented at 32nd URSI General Assembly and Scientific Symposium (GASS), Montreal, Canada. https://doi.org/10.23919/URSIGASS.2017.8104973

Xiao, S., Moore, P. J., & Judd, M. (2009). *Investigating the assessment of insulation integrity using radiometric partial discharge measurement*. Paper Presented at International Conference on Sustainable Power Generation and Supply (SUPERGEN), Nanjing, China. https://doi.org/10.1109/SUPERGEN.2009.5347978

Xu, Y., Zhou, J., & Zhang, P. (2014). RSS-based source localization when path-loss model parameters are unknown. *IEEE Communications Letters*, *18*(6), 1055–1058. https://doi.org/10.1109/LCOMM.2014.2318031

Zhang, Y., Neto, J. M., Upton, D., Jaber, A., Khan, U., Saeed, B., et al. (2015). *Radiometric monitoring system for partial discharge detection in substation*. Paper Presented at 1st URSI Atlantic Radio Science Conference (URSI AT-RASC), Gran Canaria, Spain. https://doi.org/10.1109/URSI-AT-RASC.2015.7302823

Zhang, Y., Upton, D., Jaber, A., Ahmed, H., Saeed, B., Mather, P., et al. (2015). Radiometric wireless sensor network monitoring of partial discharge in electrical substations. *Hindawi International Journal of Distributed Sensor Networks*, *11*(9), 1–9. https://doi.org/10.1155/2015/438302

Zhu, M. X., Wang, Y. B., Li, Y., Mu, H. B., Deng, J. B., Shao, X. J., & Zhang, G. J. (2016). *Detection and localization of partial discharge in air-insulated substations using UHF antenna array*. Paper Presented at 3rd IEEE Conference on Power Engineering and Renewable Energy (ICPERE), Yogyakarta, Indonesia. https://doi.org/10.1109/ICPERE.2016.7904875

Zhu, M. X., Wang, Y. B., Liu, Q., Zhang, J. N., Deng, J. B., Zhang, G. J., et al. (2017). Localization of multiple partial discharge sources in air-insulated substation using probability-based algorithm. *IEEE Transactions on Dielectrics and Electrical Insulation*, *24*(1), 157–166. https://doi.org/10.1109/TDEI.2016.005964